Supplementary Information

Sophisticatedly Structured Silica on Aggregates of Polyamine with Different Architecture

Ren-Hua Jin* and Jian-Jun Yuan
Synthetic Chemistry Lab, Kawamura Institute of Chemical Research,
631 Sakado, Sakura, Chiba 285-0078, Japan
*e-mail:jin@kicr.or.jp

Experimental section

Precursor polymers **1s-3s**

A precursor star polymer with porphyrin center **1s** [degree of polymerization of per arm = 240, determined by ^{1}H NMR relative to the porphyrin core; molecular weight distributions Mw/Mn = 1.44, determined by GPC relative to poly(ethyleneoxide) standard; RI detector; DMF as eluent] was synthesized according to our previously reported method [R.-H. Jin, *Chem. Commun.* 198-199 (2002). Also see R.-H. Jin et al., *J. Porphyrines & Phthalocyanines* 3, 6-9 (1999); R.-H. Jin., *Adv. Mater.,* 14, 889-892 (2002);; R.-H. Jin, *Macromol. Chem. Phys.* 204, 403-409 (2003); R.-H. Jin, *J. Mater. Chem.,* 14, 320-327 (2004)]. A precursor star polymer with benzene center **2s** [degree of polymerization of per arm estimated from quantitative polymerization by feeding ratio was 100, and Mw/Mn = 1.6 by GPC] was synthesized according to our previously reported method [Jin, R.-H., *J. Mater. Chem.* 13, 672-675 (2003)]. A precursor polymer **3s** (Mw =500000, Mw/Mn = 3.2) was obtained from Polyscience.

Typical hydrolysis of precursor polymer **1s** into poly(ethyleneimine) **1**:

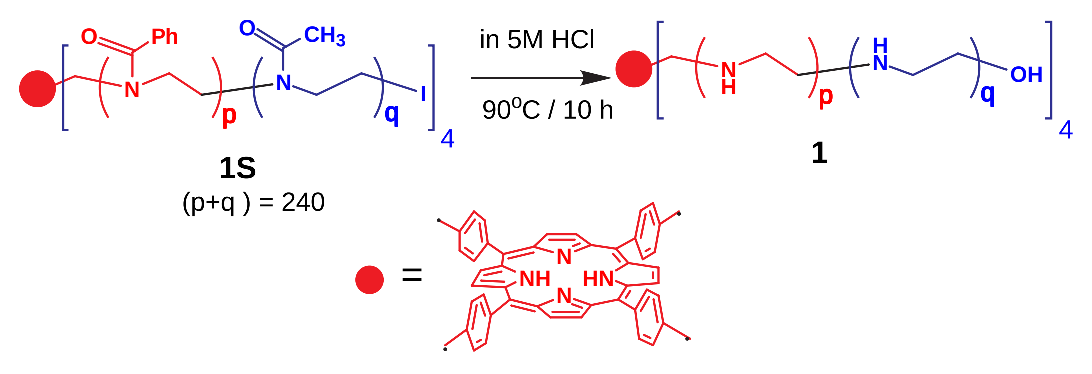

The hydrolysis was performed as follows. 0.5 g of the star **1s** was dissolved in 10 mL of 5 M HCl, and the solution was stirred at 90°C for 10 h. This hydrolysis gave insoluble precipitates. After cooling to room temperature, the mixture was filtered and solid product **1**/HCl was washed three times by acetone. The product was easily soluble in water, but not in methanol. In ^{1}H NMR (D_2O), methyl peak (2.11 ppm) due to acetyl group and phenyl peaks (7.09-7.43 ppm) due to benzoyl group disappeared and only a single peak 3.4 ppm (-NCH_2CH_2-) was observed. The powder was dissolved in water and dialyzed against 5M ammonia water for 2 days. This treatment resulted in deprotonation of PEI and yielded crystallized star **1** in dialysis tube. The crystalline solid was washed by acetone and it was dried at room temperature followed drying under vacuum at 40°C for 6h. Yield, 0.35 g. ^1H NMR (in D_2O, 80°C) showed only a single peak at 2.8 ppm.

Polymers **2** and **3** were obtained with the same manner. Since the hydrolysis of precursor poly(oxazoline)s did not break the main chain, degree of polymerization did not change after hydrolysis.

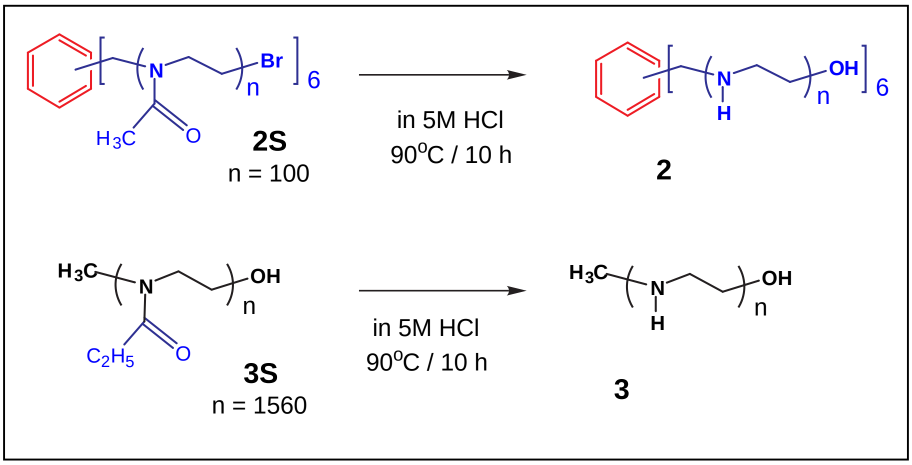

Silicification of TMOS in polymer crystalline hydrogel

Typically, 1 mL PEI hydrogel with a concentration of 2.0 % (0.48 mM of PEI repeat units) was suspended in 2 mL mixture of TMOS/ethanol (TMOS, 6.8 mM) with volume ratio of 1/1. Silica deposition almost completed by 10 min at room temperature. After left the mixture for further 30 min, the resulting silica powders were washed by acetone and centrifuged by 16000 rpm for 5 min. This was repeated three times for removing completely the excess of TMOS. The precipitate silica powders were dried at room temperature under vacuum.

Under conditions with the excess of TMOS, the yields of the silicas mediated from the PEIs aggregates increased with increasing the PEIs content. Per gram of polymers **1**, **2** and **3** could deposit respectively about 6.3, 6.1 and 5.0 g of SiO_2. It seems that the silica deposition activity of the PEI fibrils associated from the star polymers is higher than that of the linear one. The silica was characterized with ^{29}Si NMR profiles (below).

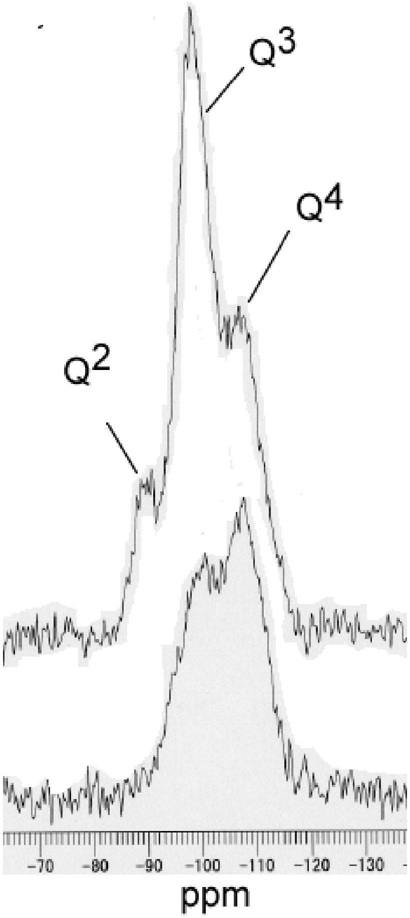

^{29}Si MAS NMR profiles of the sponge-like silica particles. The silica as prepared (bottom) and calcinated at 500ºC for 2 h (top). The silica did not change its shape after calcination. Silicate species $Si(OSi)_4$ (Q^4), $HOSi(OSi)_3$ (Q^3), and $(HO)_2Si(OSi)_2$ (Q^2) were quantified from their ^{29}Si chemical shifts at -108, -100 and -91 ppm, respectively. It is clear that a ratio of Q^4/Q^3 is >1 and no remarkable signal could be assigned to Q^2 in the fresh silica. From the spectrum of the calcinated silica, however, it is remarkable that the ratio of Q^4/Q^3 inverted dramatically being smaller than 1 and a weak and small signal due to Q^2 appeared at -91 ppm.

Measurements and characterizations

SEM images of the silicas were recorded on VE7800 (KEYENCE) and JES-6700F (JEOL) scanning electron microscopes. TEM and HR-TEM images of the silicas were obtained on JEM-200CX (JEOL) and EM-002B (TOPCON) transmission electron microscopes, respectively, without metal coating. XRD and DSC traces were recorded on Rint-Ultima (Rikagaku Co.) and DSC-7 (Perkin-Elmer) instruments, respectively. ^{29}Si MAS NMR spectra (79.3 MHz) were recorded on a GSX-400 spectrometer (JEOL), where chemical shifts were determined with respect to silicon rubber (= -22.0 ppm) as a reference.

Supporting Figures

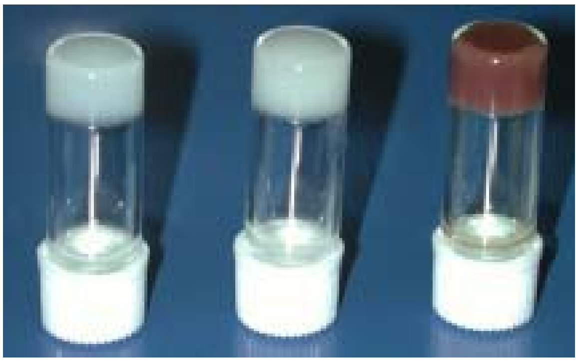

Fig. S1. Photographs of ice cream-like hydrogel aggregates containing 1% of **3, 2** and **1** (from left). These hydrogels are thermoreversible.

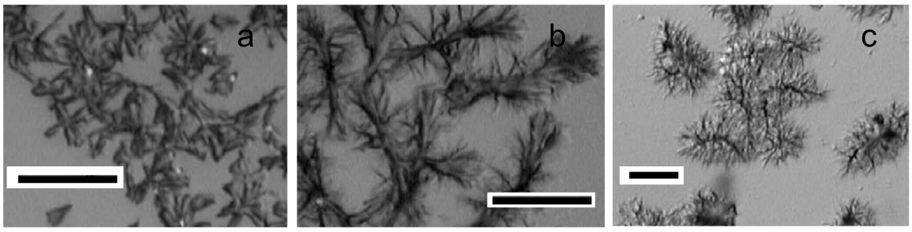

Fig. S2. Optical microscope images observed from the aqueous aggregates of polymers 1 (**a**), 2 (**b**) and 3 (**c**), scale bar 10 m. These differently shaped crystalline aggregates sustained the hydrogels shown in Fig. S1.

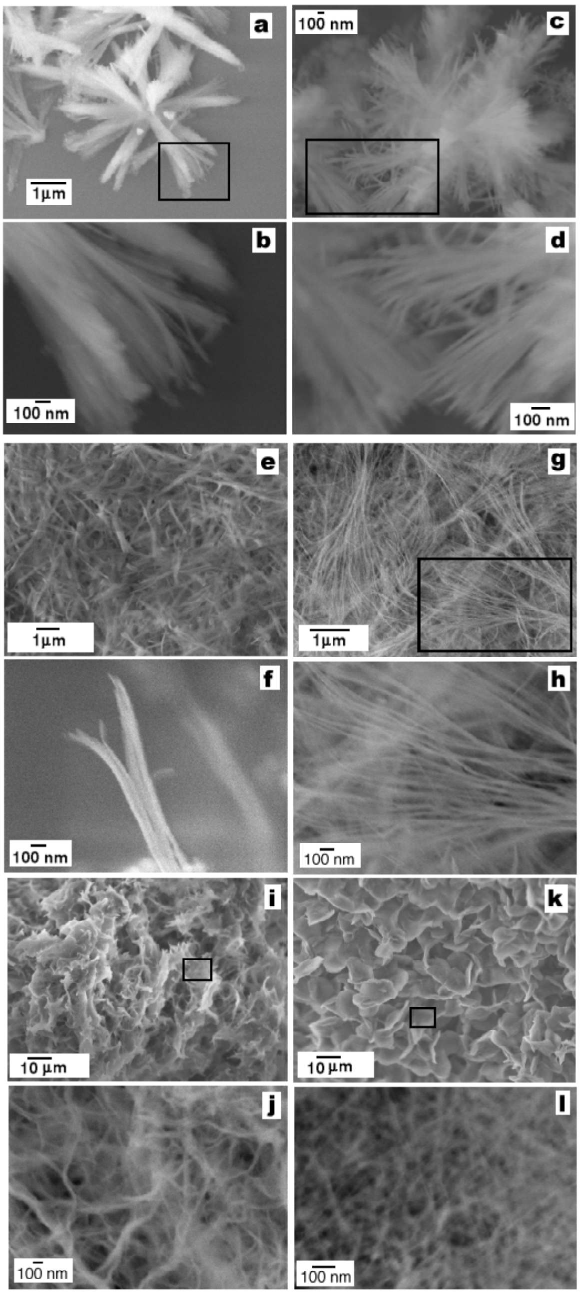

Full images of Fig 2 appeared in the main text. SEM images of the shaped silicas. The left and the right silicas were obtained at 2.0 and 0.25% concentrations of the polymers, respectively. (**a~d**) for the aster silicas, **b** and **d** are magnification images of the boxed regions in **a** and **c**, respectively; (**e~h**) for the sponge silica, **f** and **h** are magnification images in **e** and **g**, respectively; (**i~l**) for the leaf silica, **j** and **l** are magnification images of the boxed regions in **i** and **k**, respectively.

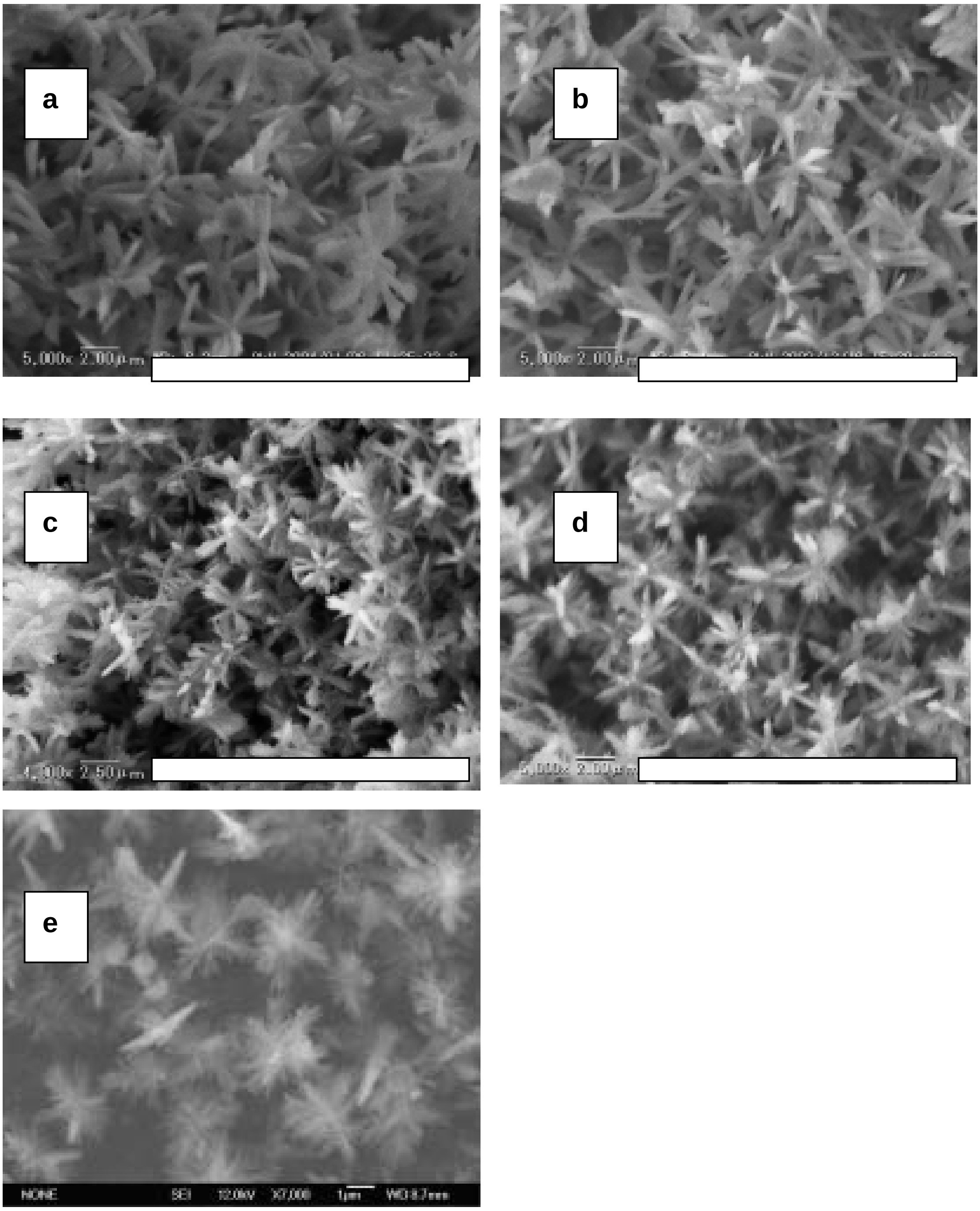

Fig. S2. SEM images of the aster-like silica mediated from different concentrations of the star polymer **1**. a) 3%, b) 2%, c) 1%, d) 0.5%, e) 0.25%.

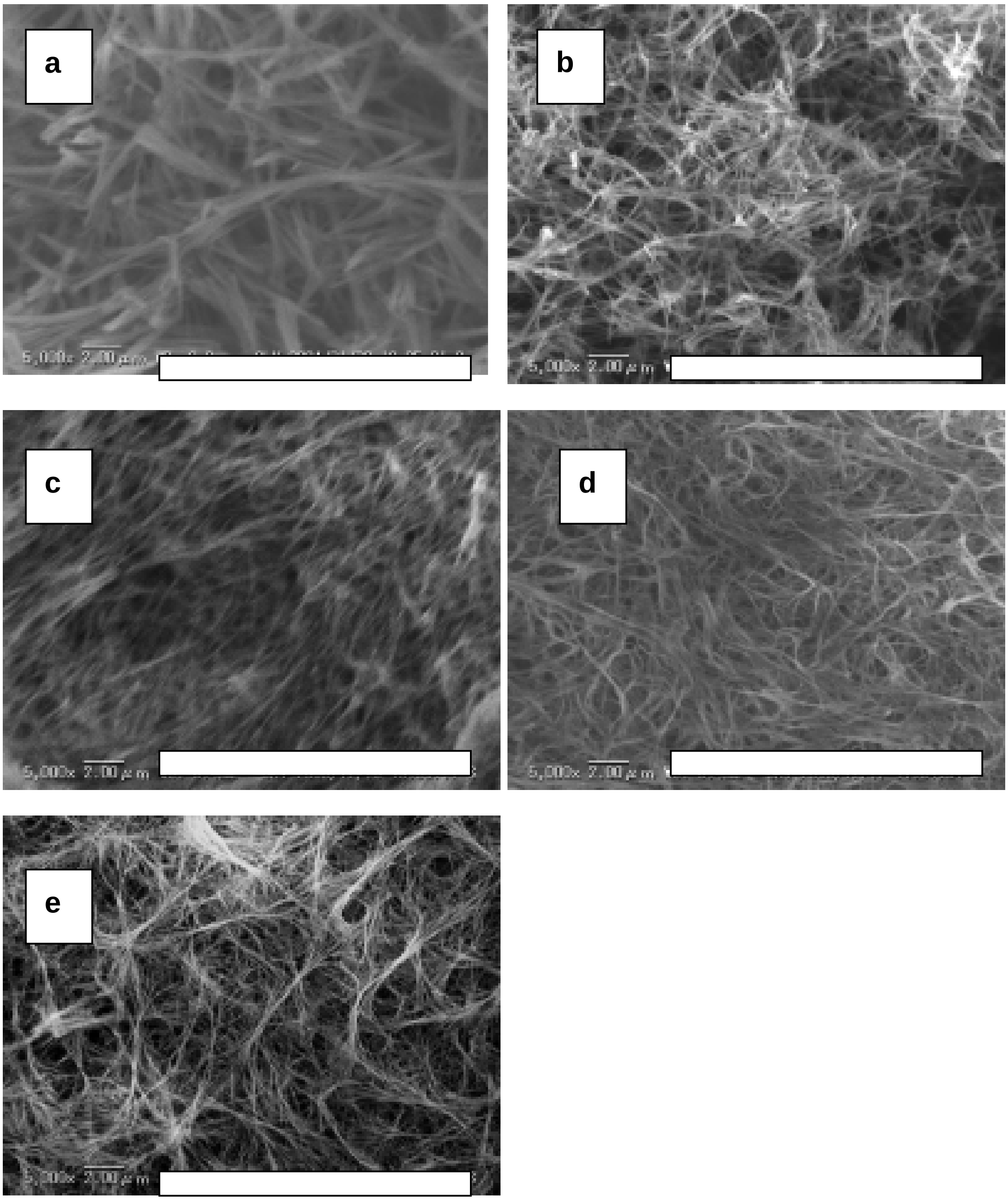

Fig. S3. SEM images of the fiber sponge-like silica mediated from different concentrations of the star polymer **2**. a) 3%, b) 2%, c) 1%, d) 0.5%, e) 0.25%.

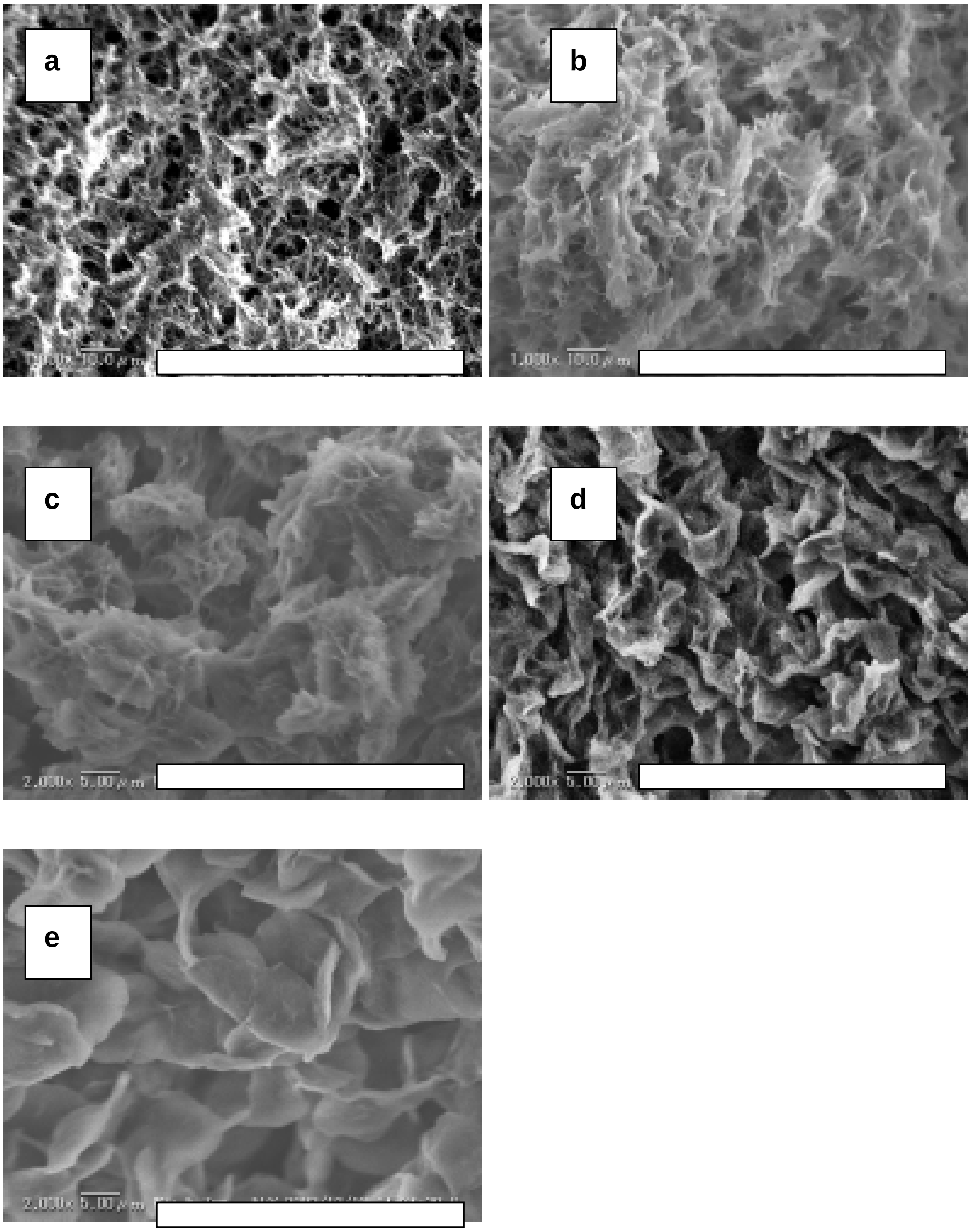

Fig. S4. SEM images of the leaf-like silica mediated from different concentrations of the linear polymer **3**. a) 3%, b) 2%, c) 1%, d) 0.5%, e) 0.25%.

From the SEM images in Figures S2-S4, it is suggestive that the crystalline filaments of the PEIs in the aqueous aggregates play the role of templates to deposit silica source around their surface, and the filaments situations in direction, entanglement and aggregation determine the final shape of the silicas. With respect to the aster silica, the contribution of the porphyrin residues in polymer **1** on shape control seems significant **(Fig. S5)**. The absorption spectra due to the porphyrin residues in **1** indicated strongly that the stacking between the porphyrin residues occurred in the silica and in the aqueous aggregate, but not occurred in a methanol solution. This is sharply contrast to our previous work (Jin, R.-H. *Chem. Commun.* 198-199, (2002)), where porphyrin residues in hollow silica, which is hybridized with porphyrin centered star poly(oxazoline), did not form stacking structure.

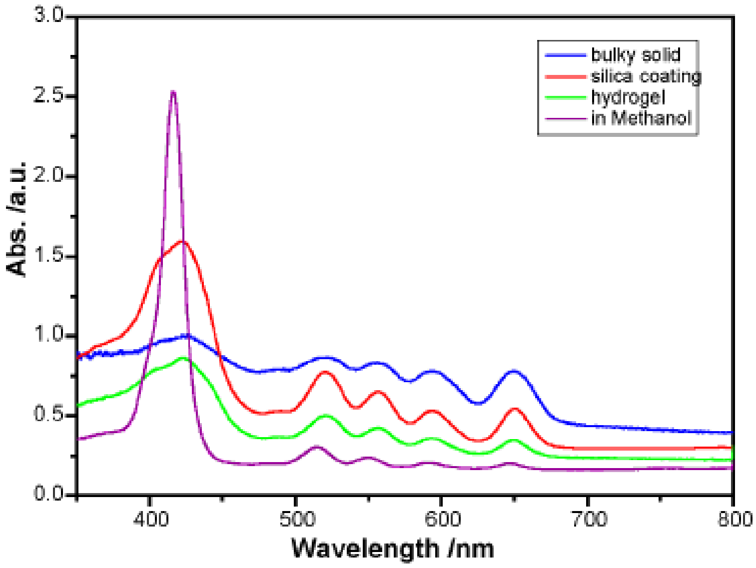

Fig. S5. UV-Vis spectra of polymer **1** in different states measured using integrating sphere attachment. Blue: solid polymer, red: spiraster silica, green: hydrogel-like aggregate, purple: in methanol solution. In the methanol solution, porphyrin residues in polymer **1** existed in isolated molecular state with sharp Soret band at 420 nm. But in the other situations, the Soret band became very broad and the four Q bands also red-shifted indicating that the porphyrin residues associated each other to from stacking aggregates.

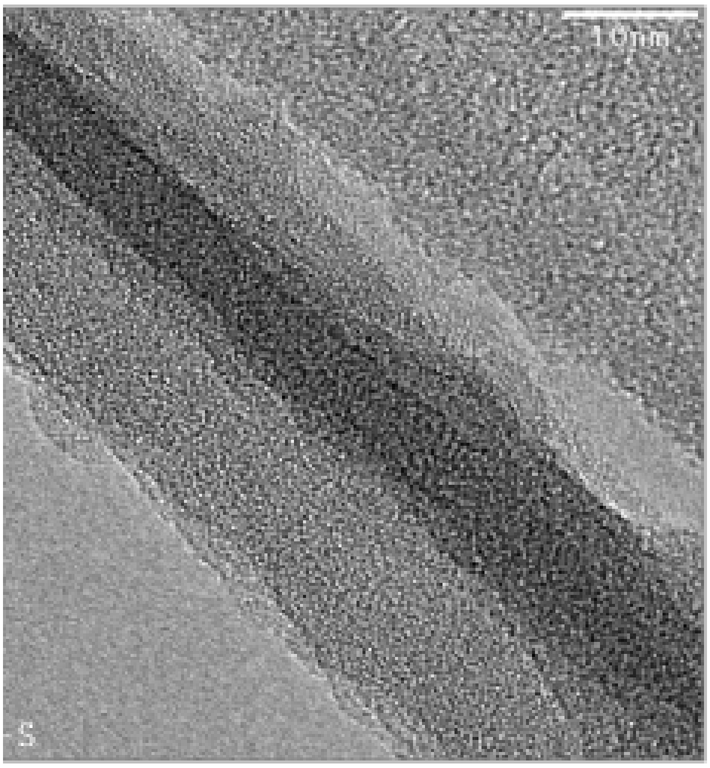

Full size HR-TEM image of Fig. 3d appeared in the main text.

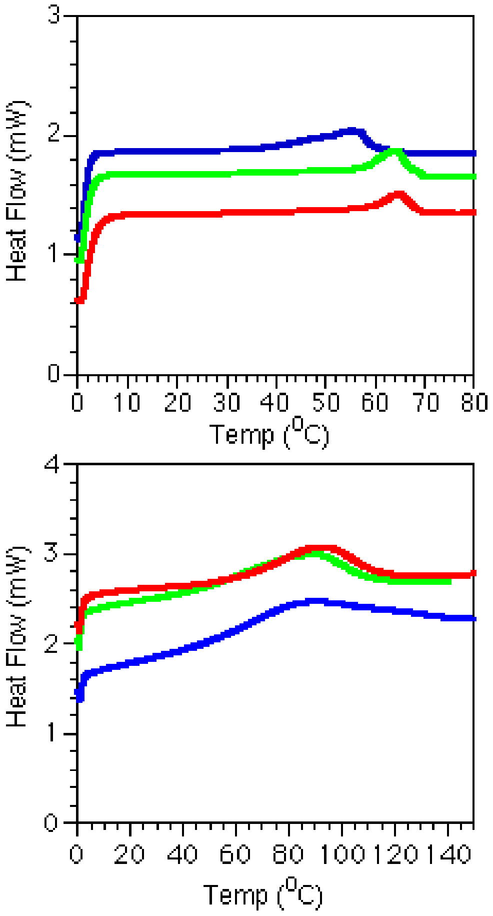

Fig. S6. DSC traces of the polymers 1-3 in the aqueous aggregates (top) and in the silicas (bottom), respectively: blue for 1; green for 2; red for 3. The aqueous aggregates showed their melting peaks at 55, 63 and 64°C, respectively, for **1**, **2** and **3**. The shaped silicas also showed melting peaks due to the enclosed PEIs. However, compared to the case of the aqueous aggregates systems, the DSC traces of the silicas showed broad endotherm lines with relatively higher temperature endotherm peaks (bottom).